JOURNAL OF CHEMICAL & ENGINEERING DATA

ARTICLE

pubs.acs.org/jced

Removal of As^V by Fe^{III}-Loaded XAD7 Impregnated Resin Containing Di(2-ethylhexyl) Phosphoric Acid (DEHPA): Equilibrium, Kinetic, and Thermodynamic Modeling Studies

Adina Negrea,[†] Mihaela Ciopec,[†] Lavinia Lupa,[*,†] Corneliu M. Davidescu,[†] Adriana Popa,[‡] Gheorghe Ilia,[‡] and Petru Negrea[†]

[†]Faculty of Industrial Chemistry and Environmental Engineering, Politehnica University, 2 Piata Victoriei, 300006, Timisoara, Romania

[‡]Institute of Chemistry Timisoara of Romanian Academy, Romanian Academy, 24 Mihai Viteazul Blv., 300223, Timisoara, Romania

ABSTRACT: In this paper, we studied the feasibility of using Fe^{III}-loaded Amberlite XAD7 impregnated resin containing di(2-ethylhexyl) phosphoric acid (DEHPA) as adsorbents for the removal of As^V from aqueous solution. The XAD7-DEHPA resins are obtained by the dry method (DM) and column method (CM) of impregnation, respectively. Equilibrium, kinetic, and thermodynamic studies are carried out to study the adsorption performance of both types of Fe-XAD7-DEHPA resins for the removal process of As^V from aqueous solution. The effects of initial As^V concentration, contact time, and temperature of the solution on the adsorption were studied. The Langmuir and Dubinin−Kaganer−Radushkevich (DKR) isotherm models fit the equilibrium data better than Freundlich and Temkin isotherm models, which are used to describe the adsorption of As^V onto Fe-XAD7-DEHPA resins. The pseudosecond-order model is suitable for describing the adsorption kinetics for As^V removal from aqueous solutions onto Fe-XAD7-DEHPA resins. Thermodynamic parameters, such as the Gibbs energy ($\Delta G^{\#}$), enthalpy ($\Delta H^{\#}$), entropy ($\Delta S^{\#}$), and equilibrium constant of activation ($K^{\#}$) are calculated. The adsorption capacities of the both studied materials are found to be almost the same. However, the Fe-XAD7-DEHPA obtained through the CM is the most advantageous as this is obtained in a shorter time than the resin obtained through the DM.

INTRODUCTION

The presence of dissolved arsenic in groundwater has created significant concern on a global basis. The consumption of arsenic-containing water causes serious health-related problems because of its toxicity.[1−6] Thus, choosing a technology for the removal of arsenic from drinking water represents a challenge.

The chemistry of arsenic in aquatic systems is complex and consists of oxidation−reduction, precipitation, adsorption, and ligand exchange. The principal aqueous forms of inorganic arsenic are arsenate [As^V] and arsenit [As^{III}], and their relative distributions are influenced by pH and redox conditions.[5−8] As^V species are found in oxidizing environments at a pH between 6 and 9 as oxyanions of arsenic acid [$H_2AsO_4^-$ or $HAsO_4^{2-}$],[3,8,9] while As^{III} species exist as uncharged arsenious acid [$H_3AsO_3^0$] at pH below 9.[3,8,10]

A literature survey reveals that there are a good number of approaches for arsenic remediation from drinking water. Among the various methods like oxidation−reduction, precipitation, coagulation and coprecipitation, adsorption, electrolysis and cementation, solvent extraction, ion exchange, ion flotation, biological processing, and membrane filtration[1,2,8,9,11−19] proposed to negotiate the problem of arsenic contamination in drinking water, the sorption technique is, however, the most common and is considered to be an effective method. This method is simple and convenient and also has the potential for regeneration and a sludge-free operation.

To date, various adsorbents like metal oxides/hydroxides,[6,8,9,12,20−25] natural and synthetic zeolites,[7,20] laterite soil,[12,20,26] calcite,[27] and activated carbon[2,3,20,28] have been developed for arsenic removal.

The adsorption in porous solid adsorbent is a complex process with respect to the nature of the solid adsorbent surface adsorbate.[29] The use of macroporous organic polymer supports, with a high specific surface area and good mechanical stability, is found to be more suitable for the removal of toxic elements from dilute solution, due to their faster kinetics, ease of regeneration, and high adsorption capacity.[30−38] Impregnating appropriate solid supports, such as Amberlite XAD series, is one of the well-known and effective solid sorbent preparation methods for treatment purposes.[20,30,32,33,35] There are four methods available for the impregnation of the desired extractant into the polymeric supporting structure: the dry method (DM), wet method, modifier addition method, and dynamic column method (CM).[34,39−42]

The most widely used method of impregnation, cited in literature, is the DM, while the CM is very rarely mentioned. In the present work a comparison between the adsorption performance of the XAD7 resin impregnated with di(2-ethylhexyl) phosphoric acid (DEHPA) through the DM and the adsorption performance of XAD7 resin impregnated through CM in the process of As^V ion removal from aqueous solutions was studied. Because the iron compounds in general were found to be very efficient adsorbents for arsenic removal from water, due to the high affinity of arsenic toward iron,[1,4−6,8,12,23,28,37,43] the XAD7 resins impregnated with DEHPA, employing the both mentioned methods, were loaded with Fe^{III} ions.

Received: May 15, 2011
Accepted: August 12, 2011
Published: August 26, 2011

Due to the fact that the column method of impregnation (CM, an effective method of impregnation, which is not studied and cited in the specialty literature) needs a lower time of impregnation than the DM of impregnation, the objective of this study is to determine and compare the adsorption performances of the Fe-XAD7-DEHPA resins (obtained via the both mentioned methods of impregnation) in the removal process of As^V from aqueous solutions. To determine the adsorption performances of Fe-XAD7-DEHPA resins, equilibrium, kinetic, and thermodynamic studies were performed.

MATERIALS AND METHODS

Adsorbent Preparation. The Amberlite XAD7 resin (supplied by Rohm and Hass Co.) was impregnated with DEHPA through the DM and CM. The DEHPA (~ 98.5 %) used as the extractant was supplied by BHD Chemicals Ltd. (Poole, England) and used as received. For the DM impregnation 1 g of fresh XAD7 was placed for 24 h in ethanol containing 0.1 $g \cdot mL^{-1}$ extractant (DEHPA). The polymeric beads were separated through a porous filter using a vacuum pump, washed with water, and dried at 323.15 ± 1 K for 24 h.[41] For the Amberlite XAD7 resin impregnation with DEHPA and ethylic alcohol as solvent by the dynamic column impregnation method,[41] a certain amount of polymer fully swollen by the solvent was packed in a glass column of 4 cm diameter and 15 cm height. Then the extractant solution was fed into the column with a 0.1 $L \cdot h^{-1}$ flow rate until the extractant (at the outlet) and feed concentrations were equal. The polymeric beads were separated through a porous filter using a vacuum pump, washed with water, and dried at 323.15 ± 1 K for 24 h.[42] The resulting SIRs were finally washed with distilled water. The extractant content of the impregnated resins was determined after washing a given amount of the resins with ethanol, which completely elutes the ligand and subsequent titration with 0.1 M NaOH.

In this form the XAD7-DEHPA resins are anionic resins, which can be used as adsorbents for divalent and trivalent metal ion removal from aquatic solutions. They cannot be used for the removal of anionic species of arsenate from water. From this reason a metal ion like iron, manganese, zirconium, or aluminum must be loaded on the XAD7-DEHPA resins. The best metal ion for the arsenic removal is considered to be the iron ion because of the high affinity of Fe toward inorganic arsenic.[1,4−6,8,12,23,25,28,37,43] Therefore, the XAD7 resins impregnated with DEHPA through DM and CM were loaded with Fe^{III} ions ($Fe(NO_3)_3$ in 0.5 $mol \cdot L^{-1}$ HNO_3 solution). In this aim 5 g of each XAD7-DEHPA resins was equilibrated with 200 mL of 50 $mg \cdot L^{-1}$ Fe^{III} solution for 24 h. Fe-XAD7-DEHPA resins were separated through a porous filter using a vacuum pump, washed with distilled water until pH was neutral, and dried at 323.15 ± 1 K for 24 h. The residual concentration of the Fe^{III} ions in the resulting solutions after filtration has been determined using a Varian SpectrAA 280 fast sequential atomic absorption spectrometer with an air-acetylene flame.

Adsorption Experiments. The experiments were performed with both resins at an initial pH of As^V solution of 9 ± 0.1, because the predominant anionic species of As^V [$H_2AsO_4^-$ or $HAsO_4^{2-}$] are found in the environment samples at this pH value.[3,8,9] The pH of the solutions was adjusted to this value using a 1 M NaOH solutions, thereby keeping the volume variation of the solution to a value as low as possible. The pH of the solutions was measured via a CRISON MultiMeter MM41 fitted with a glass electrode which had been calibrated using various buffer solutions.

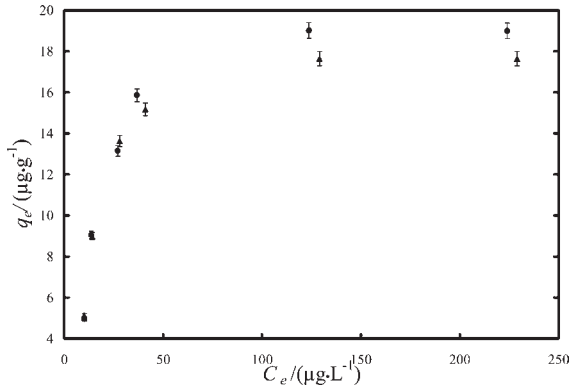

Figure 1. Adsorption isotherm of As^V ions onto Fe-XAD7-DEHPA resins C_0 = (30 ± 0.01 to 300 ± 0.01) $\mu g \cdot L^{-1}$; m = 0.1 ± 0.0001 g; V = 25 ± 0.1 mL; t = 10 h; T = 298.15 ± 1 K; pH = 9 ± 0.1; ▲, DM; ●, CM. Error bars represent the relative standard deviation.

Prior to such experiments, a stock solution of arsenic was prepared by diluting an appropriate amount of H_3AsO_4 in 0.5 M HNO_3 solution (Merck Standard Solutions). Other solutions of As^V ions were prepared from the stock solution by appropriate dilution.

In the first instance, the effect of the initial As^V concentration (C_0 = (30 ± 0.01 to 300 ± 0.01) $\mu g \cdot L^{-1}$) was studied. In each experiment 0.1 ± 0.0001 g of sorbent was suspended in 25 ± 0.1 mL of As^V solution of different concentrations. The samples were kept in contact for 10 h at room temperature, 298.15 ± 1 K. The filtrate was collected for As^V analysis.

To study the effect of contact time on adsorption at three temperatures 298.15 ± 1 K, 303.15 ± 1 K, and 318 ± 1 K, the experiments were carried out with samples of 0.1 ± 0.0001 g of Fe-XAD7-DEHPA in 25 ± 0.1 mL of 100 ± 0.01 $\mu g \cdot L^{-1}$ As^V solutions. The suspensions were kept in contact for different times: (1, 2, 4, 6, 8, 10, and 24) h. To maintain the temperature of the suspensions at the desired value, the samples were immersed in a bath of a mechanical shaker bath (without shaking) MTA Kutesz 609/A, Hungary with a standard thermocouple. After contact time elapsed, the suspensions were filtered, and the residual concentration of As^V ions in the filtrates was determined by means of atomic absorption spectrometry using a Varian SpectrAA 110 atomic absorption spectrometer with a Varian VGA 77 hydride generation system.

The various chemicals employed in the experiments were of analytical reagent (A.R.) grade and used without further purification. Distilled water was used throughout. The adsorption performance is expressed as metal uptake, $q_e/\mu g \cdot g^{-1}$, and the corresponding mass balance expression is:[3,9,22,34,38,44]

$$q_t = \frac{(C_0 - C_t) \cdot V}{m} \quad (1)$$

where C_0 and C_t are the concentrations of As^V ions ($\mu g \cdot L^{-1}$) in the solution initially (t = 0) and after a time t (h), respectively, V is the volume of the solution (V = (25 ± 0.1) · 1000^{-1} L), and m is the mass of adsorbent (m = 0.1 ± 0.0001 g). The experimental results are given as an average of five sets of data obtained in identical working conditions.

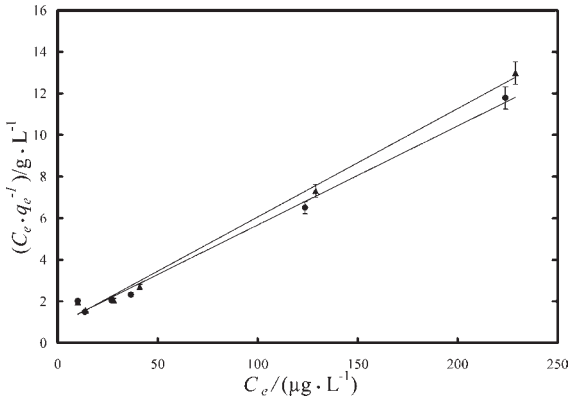

Figure 2. Langmuir plot of As^V adsorption onto Fe-XAD7-DEHPA resins: ▲, DM; ●, CM. Error bars represent the average relative error.

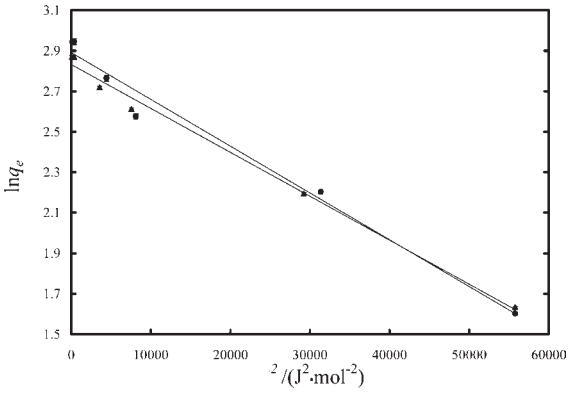

Figure 3. Dubinin−Kaganer−Radushkevich plot of As^V adsorption onto Fe-XAD7-DEHPA resins; ▲, DM; ●, CM. Error bars represent the average relative error.

RESULTS AND DISCUSSION

The extractant content of the XAD7-DEHPA obtained through the DM of impregnation determined by titration with 0.1 M NaOH was 0.35 g DEHPA/g SIR, and the extractant content of the XAD7-DEHPA obtained through the CM of impregnation was 0.352 g DEHPA/g SIR. The analysis of the residual concentration of the Fe^{III} in the resulting solution after filtration showed that the entire quantity of Fe^{III} ions from the solutions was loaded on the studied resins.

Concentration Dependence and Adsorption Isotherms. The adsorption isotherm for As^V ions onto Fe-XAD7-DEHPA resins are presented in Figure 1.

The adsorption capacity increased with increasing equilibrium concentration of arsenic for the both studied resins. Then, it approached a constant value at the high equilibrium concentrations. One can be observed that the Fe-XAD7-DEHPA obtained through DM develops a maximum adsorption capacity of As^V of 17.6 $\mu g \cdot g^{-1}$, while the maximum adsorption capacity of As^V developed by the Fe-XAD7-DEHPA obtained via CM is 19 $\mu g \cdot g^{-1}$.

Four important isotherm models were chosen to fit the experimental data in this study: Langmuir, Freundlich, Temkin, and Dubinin−Kaganer−Radushkevich.

The linear form of the Langmuir equation[2−7,9,22−25,35,37,38] is expressed by:

$$\frac{C_e}{q_e} = \frac{1}{K_L q_m} + \frac{C_e}{q_m} \tag{2}$$

where K_L denotes the Langmuir isotherm constant related to the affinity between adsorbent and the adsorbate ($L \cdot \mu g^{-1}$) and q_m denotes the Langmuir monomolecular adsorption capacity ($\mu g \cdot g^{-1}$). The values of q_m and K_L can be determined by plotting $C_e \cdot q_e^{-1}$ versus C_e (Figure 2).

The Freundlich isotherm[2−7,9,22,23,25,35,37,38] equation can be written as:

$$\ln q_e = \ln K_F + \frac{1}{n} \cdot \ln C_e \tag{3}$$

where q_e is the amount of As^V adsorbed per gram of adsorbent, that is, metal uptake ($\mu g \cdot g^{-1}$), and C_e is the equilibrium concentration of adsorbate in the bulk solution after adsorption ($\mu g \cdot L^{-1}$). K_F and $1/n$ are characteristic constants that can be related to the relative adsorption capacity of the adsorbent ($\mu g \cdot g^{-1}$) and the intensity of the adsorption, respectively, and can be determined from the plot of ln q_e versus ln C_e.

The equation of the Temkin model[44,45] is given by:

$$q_e = \left(\frac{RT}{b_T}\right) \cdot \ln K_T + \left(\frac{RT}{b_T}\right) \cdot \ln C_e \tag{4}$$

where b_T is the adsorption potential of the adsorbent and K_T is the equilibrium constant corresponding to maximum binding energy ($L \cdot \mu g^{-1}$), R is the universal gas constant ($J \cdot (mol \cdot K)^{-1}$), and T is the absolute temperature (K).

K_T, determined from the plot of q_e versus ln C_e, can be used to determine the value of the standard free enthalpy $\Delta G°$ as follows:

$$K_T = \exp\left(\frac{-\Delta G^0}{RT}\right) \tag{5}$$

The Dubinin−Kaganer−Radushkevich (DKR) isotherm equation[2] is based on the concept of heterogeneous surface of the adsorbent and can be written as:

$$\ln q_e = \ln q_m - \beta \cdot \varepsilon^2 \tag{6}$$

where the quantities q_e and q_m are the amount of As^V adsorbed per gram of adsorbent, that is, metal uptake ($\mu g \cdot g^{-1}$) and the measurement of the monolayer adsorption capacity ($\mu g \cdot g^{-1}$), respectively. β is the activity coefficient related to the mean sorption energy, and ε is the Polanyi potential and can be calculated using the following relation:

$$\varepsilon = RT \ln\left(1 + \frac{1}{C_e}\right) \tag{7}$$

where R is the universal gas constant, T is the temperature in Kelvin, and C_e is the equilibrium concentration of adsorbate in the bulk solution after adsorption ($\mu g \cdot L^{-1}$).

A plot of ln q_e versus ε^2 (Figure 3) yields a straight line, confirming the model. The mean free energy of adsorption E ($kJ \cdot mol^{-1}$) per molecule of the adsorbate when it is transferred from the solution to the powder surface can be calculated using the following equation:[2]

$$E = \frac{1}{\sqrt{2\beta}} \tag{8}$$

dx.doi.org/10.1021/je200476u |J. Chem. Eng. Data 2011, 56, 3830–3838

Table 1. Parameters of Different Isotherms for As^V Ion Adsorption onto Fe-XAD7-DEHPA Resins

isotherm	adsorbent Fe-XAD7-DEHPA	isotherm parameters			R^2	Δq/%	E/%
Langmuir		$K_L/(L\cdot\mu g^{-1})$	q_m (calc.)/($\mu g\cdot g^{-1}$)				
	DM	0.062	19.2		0.9943	20.5	4.2
	CM	0.052	21.0		0.9919	21.3	4.5
Freundlich		$K_F/(\mu g\cdot g^{-1})$	$1/n$				
	DM	3.395	0.3396		0.7413	26.5	7.0
	CM	3.136	0.3711		0.7562	28.1	7.9
Temkin		$K_T/(L\cdot mol^{-1})$	$\Delta G°/(kJ\cdot mol^{-1})$				
	DM	0.775	0.63		0.8496	24.9	6.2
	CM	0.585	1.33		0.8745	25.8	6.7
DKR		$\beta/(mol^2\cdot J^{-2})$	q_m(calc.)/($\mu g\cdot g^{-1}$)	$E/(kJ\cdot mol^{-1})$			
	DM	$2.2\cdot10^{-5}$	17	0.15	0.9929	4.2	0.2
	CM	$2.3\cdot10^{-5}$	18	0.147	0.9814	7.4	0.5

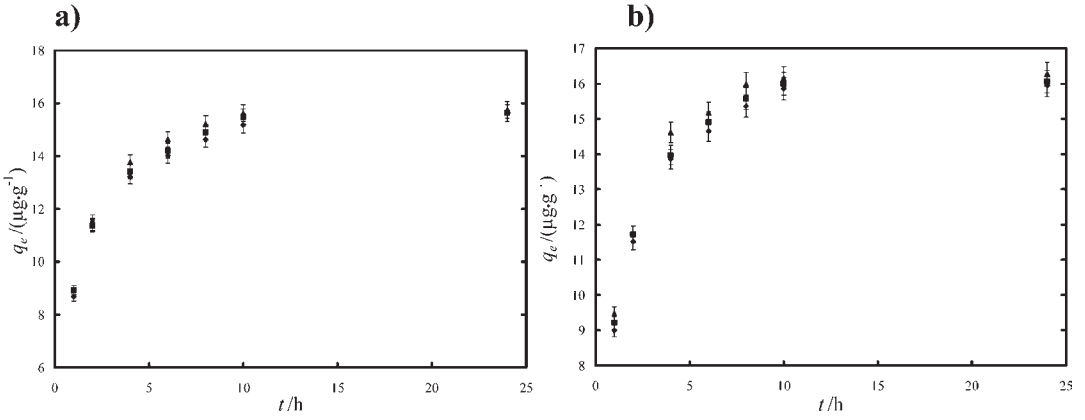

Figure 4. Effect of contact time on the adsorption capacity of the studied materials at different temperatures; $C_0 = 100 \pm 0.01\ \mu g\cdot L^{-1}$; $m = 0.1 \pm 0.0001$ g; $V = 25 \pm 0.1$ mL; pH = 9 ± 0.1; a, DM; b, CM; ♦, 298.15 ± 1 K; ■, 303.15 ± 1 K; ▲, 318.15 ± 1 K. Error bars represent the relative standard deviation.

The isotherm equation parameters of Langmuir, Freundlich, Temkin, and Dubinin−Kaganer−Radushkevich are summarized in Table 1.

To assess the extent to which the adsorption isotherm equations fit the experimental data, two different error functions were examined.

The normalized standard deviation Δq/% was estimated using the equation:[4,46,47]

$$\Delta q = 100\cdot\sqrt{\frac{1}{p-1}\sum_{i=1}^{p}\left(\frac{q_{exp}-q_{calc}}{q_{exp}}\right)_i^2} \quad (9)$$

where q_{exp} is the experimentally determined adsorption capacity ($\mu g\cdot g^{-1}$), q_{calc} is the adsorption capacity calculated according to the model equation ($\mu g\cdot g^{-1}$), and p is the number of experimental data.

The average relative error E/%, which minimizes the fractional error distribution across the entire concentration range, was estimated with the equation:[4,48]

$$E = \frac{100}{p-1}\cdot\sum_{i=1}^{p}\left(\frac{q_{calc}-q_{exp}}{q_{exp}}\right)_i^2 \quad (10)$$

An analysis of R^2 and of the absolute error values (Table 1) showed that the Langmuir and Dubinin−Kaganer−Radushkevich equations have more precise coefficients and lower absolute error than the Freundlich and Temkin equations for modeling the As^V adsorption onto Fe-XAD7-DEHPA resins obtained through DM and CM, respectively.

The Langmuir adsorption isotherm provided an excellent fit to the equilibrium adsorption data, giving correlation coefficients >0.99 and maximum adsorption capacities close to that determined experimentally. The maximum adsorption capacity of the Fe-XAD7-DEHPA resin obtained through the CM is higher than the maximum adsorption capacity of the Fe-XAD7-DEHPA resin obtained through the DM (Table 1). The essential feature of the Langmuir equation can be expressed in terms of a dimensionless separation factor, R_L, defined as:

$$R_L = \frac{1}{1 + K_L\cdot C_0} \quad (11)$$

The value of R_L indicates the shape of the isotherm to be unfavorable, $R_L > 1$; linear, $R_L = 1$; favorable $0 < R_L < 1$; and irreversible, $R_L = 0$.[2−4,28,30,32] R_L values were found to be between 0 and 1 for all of the concentrations of As^V ions and for both studied materials, showing that the adsorption is favorable.

dx.doi.org/10.1021/je200476u |J. Chem. Eng. Data 2011, 56, 3830–3838

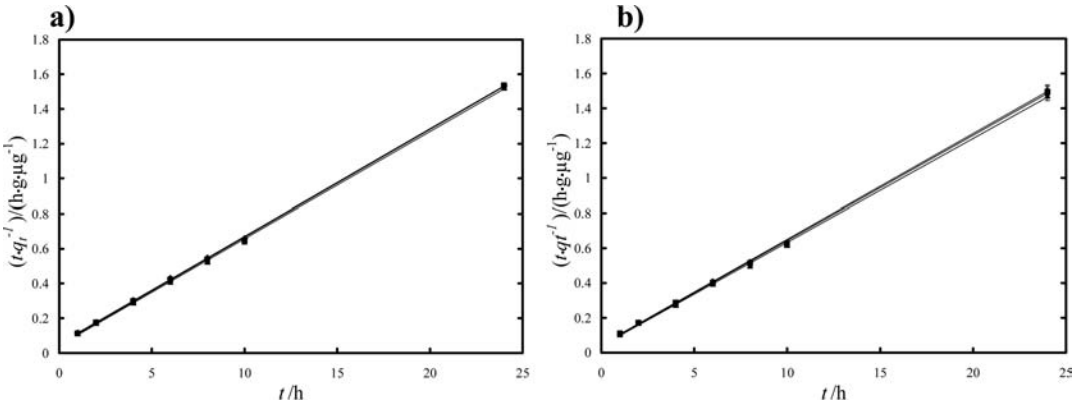

Figure 5. Pseudosecond-order kinetic plot for the adsorption of As^V onto studied materials; a, DM; b, CM; ♦, 298.15 ± 1 K; ■, 303.15 ± 1 K; ▲, 318.15 ± 1 K. Error bars represent the average relative error.

The Langmuir model indicates a homogeneous and monomolecular adsorption mechanism.

The Freundlich plots have a correlation coefficient very low; this suggests a restriction on the use of Freundlich isotherms. The constant K_F can be defined as an adsorption coefficient which represents the quantity of adsorbed metal ions for a unit equilibrium concentration. The slope $1/n$ is a measure of the adsorption intensity or surface heterogeneity. For $1/n = 1$, the partition between the two phases is independent of the concentration. The situation $1/n < 1$ is the most common and corresponds to a normal L-type Langmuir isotherm, while $1/n > 1$ indicates a cooperative adsorption, which involves strong interactions between the molecules of adsorbate.[45] Values of $1/n < 1$ indicate a very high affinity of the both Fe-XAD7-DEHPA resins for As^V ions.

The Temkin isotherm model was chosen to determine the adsorption potentials of the adsorbents for adsorbates. The Temkin adsorption potentials K_T is 0.775 $L\cdot mol^{-1}$ for Fe-XAD7-DEHPA obtained by DM and 0.585 $L\cdot mol^{-1}$ for Fe-XAD7-DEHPA obtained by CM, respectively. The values for the standard free enthalpy, $\Delta G°$, were calculated according to eq 5 for both studied materials (Table 1). These results show that, in the Temkin isotherm model, the binding energy is higher for the adsorbent obtained employing the CM than the binding energy for the adsorbent obtained through the DM. However, the Temkin model is not able to describe the experimental data properly because of the poor linear correlation coefficients.

The Dubinin−Kaganer−Radushkevich model (which presents the lowest absolute errors) was used to determine the characteristic porosity and the apparent free energy of adsorption. The monomolecular adsorption capacities q_m for Fe-XAD7-DEHPA obtained through DM and for Fe-XAD7-DEHPA obtained through CM were 17 and 18 $\mu g\cdot g^{-1}$, respectively; values which are very close to that determined experimentally. The values of the porosity factors β less than unity (Table 1) imply that Fe-XAD7-DEHPA resins consist of fine micropores and indicate a surface heterogeneity may arise from the pore structure as well as adsorbate−adsorbent interaction.[44] The apparent free energy from the Dubinin−Kaganer−Raduskevich is a parameter used in predicting the type of adsorption. If the value of E is between (8 and 16) $kJ\cdot mol^{-1}$, then the adsorption process follows by chemical ion exchange, and if $E < 8$ $kJ\cdot mol^{-1}$, the adsorption process is of a physical nature.[7,42] The apparent free energy values for the studied materials are in the region of 0.15 $kJ\cdot mol^{-1}$; these results indicate that the adsorption of As^V onto Fe-XAD7-DEHPA resins is governed by physisorption.

Contact Time Dependence and Adsorption Kinetics. The effects of contact time on equilibrium adsorption capacities of As^V for the studied materials at (298.15 ± 1, 303.15 ± 1, and 318.15 ± 1) K are presented in Figure 4.

Both materials reached the saturation level in approximately 10 h. At the initial As^V concentration of 100 ppb, the equilibrium adsorption capacities were determined to be (15.7 and 16) $\mu g\cdot g^{-1}$ of As^V adsorption onto Fe-XAD7-DEHPA obtained via DM and Fe-XAD7-DEHPA obtained via CM in 10 h, respectively. After 10 h of contact between adsorbent and adsorbate, the adsorption capacity hardly changed during the adsorption time.

The experimental kinetic data of the adsorption studies were used in the Lagergren pseudofirst-order, pseudosecond-order, and intraparticle diffusion models. The integrated forms of the models are shown below:

The pseudofirst-order kinetic model is defined by the equation:[3,9,14,25,32,35,37,38,45,49]

$$\ln(q_e - q_t) = \ln q_t - k_1\cdot t \tag{12}$$

where q_e and q_t are the amount of the As^V adsorbed onto the studied materials ($\mu g\cdot g^{-1}$) at equilibrium and at time t, respectively. t is the contact time (h), and k_1 is the specific sorption rate constant (h^{-1}). The values of the adsorption rate constant (k_1) were determined from $\ln(q_e - q_t)$ in terms of t.

The linear form of the pseudosecond-order model is defined by:[3,6,7,9,14,25,32,35,37,38,44,49]

$$\frac{t}{q_t} = \frac{1}{k_2\cdot q_e^{\,2}} + \frac{t}{q_e} \tag{13}$$

where q_e and q_t are the amount of the As^V adsorbed onto the studied materials ($\mu g\cdot g^{-1}$) at equilibrium and at time t, respectively. t is the contact time (h), and k_2 is the pseudosecond-order adsorption rate constant ($g\cdot\mu g^{-1}\cdot h^{-1}$). The values q_e and k_2 are determined from the slope and intercept of $(t\cdot q_t^{-1})$ versus t (Figure 5). In eq 13, the expression $k_2\cdot q_e^{\,2}$ in the intercept term describes the initial sorption rate $h/(\mu g\cdot(g\cdot h)^{-1})$ as $t\rightarrow 0$.

Intraparticle Diffusion Model. The adsorption of As^V ions onto the studied materials may be controlled via external film diffusion at earlier stages and later by the particle diffusion. The possibility of intraparticle diffusion resistance was identified by

Table 2. Kinetic Parameters for As^V Ion Adsorption onto Fe-XAD7-DEHPA Resins

	q_{exp}	k_1	q_{calc}		Δq	E
	$\mu g \cdot q^{-1}$	h^{-1}	$\mu g \cdot g^{-1}$	R^2	%	%
pseudofirst-order						
		$T = 298.15 \pm 1$ K				
DM	15.7	0.1907	5.69	0.9647	11.1	1.2
CM	16.0	0.2143	4.74	0.8577	15.3	2.3
		$T = 303.15 \pm 1$ K				
DM	15.7	0.1937	4.81	0.8796	13.5	1.8
CM	16.3	0.1547	4.05	0.7494	17.1	2.9
		$T = 318.15 \pm 1$ K				
DM	15.8	0.2108	4.58	0.8764	15.2	2.3
CM	16.5	0.1439	3.64	0.7202	18.2	3.3
pseudosecond-order						
	q_{exp}	k_2	q_{calc}		Δq	E
	$\mu g \cdot g^{-1}$	$g \cdot \mu g^{-1} \cdot h^{-1}$	$\mu g \cdot g^{-1}$	R^2	%	%
		$T = 298.15 \pm 1$ K				
DM	15.7	0.0719	16.2	0.9999	0.97	0.01
CM	16.0	0.0819	16.5	0.9996	3.2	0.10
		$T = 303.15 \pm 1$ K				
DM	15.7	0.0799	16.2	0.9997	2.06	0.04
CM	16.3	0.0861	16.6	0.9995	3.5	0.12
		$T = 318.15 \pm 1$ K				
DM	15.8	0.0873	16.3	0.9996	3.69	0.13
CM	16.5	0.0961	16.8	0.9994	5.6	0.31
intraparticle diffusion model						
	q_{exp}	K_{dif}			Δq	E
	$\mu g \cdot g^{-1}$	$\mu g \cdot g^{-1} \cdot h^{-1/2}$	C	R^2	%	%
		$T = 298.15 \pm 1$ K				
DM	15.7	1.6032	9.11	0.7346	11.6	1.3
CM	16.0	1.6695	9.51	0.6903	12.4	1.5
		$T = 303.15 \pm 1$ K				
DM	15.7	1.6126	9.32	0.7139	12.1	1.5
CM	16.3	1.6497	9.71	0.6927	12.1	1.4
		$T = 318.15 \pm 1$ K				
DM	15.8	1.6168	9.54	0.6776	12.6	1.6
CM	16.5	1.6426	10.0	0.6580	12.3	1.5

using the following intraparticle diffusion model:[3,9,14,44]

$$q_t = k_{dif} \cdot t^{1/2} + C \quad (14)$$

where K_{dif} is the intraparticle diffusion rate constant ($\mu g \cdot g^{-1} \cdot h^{-1/2}$) and C is the intercept. The values of q_t versus $t^{1/2}$ and the rate constant K_{dif} are directly evaluated from the slope of the regression line.

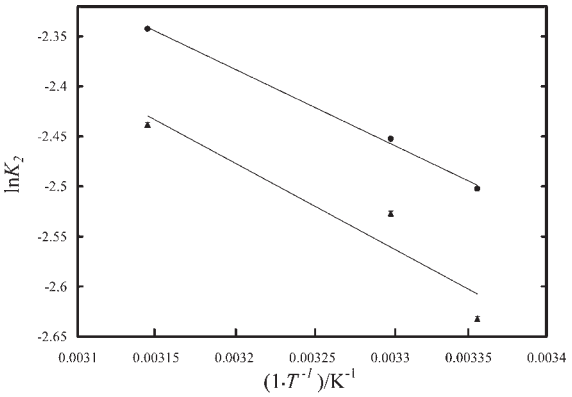

Figure 6. Arrhenius plots for the adsorption of As^V onto Fe-XAD7-DEHPA resins; ▲, DM; ●, CM. Error bars represent the relative standard deviation.

The models were tested by the normalized standard deviation (eq 9) and average relative error (eq 10) to determine which equation best describes the data. The values of the constants, together with the regression coefficients (R^2) and the absolute error values obtained in all the cases, are summarized in Table 2.

The only plot exhibiting good linearity with a good correlation coefficient (close to 1) and the lower value of the estimated errors was obtained for the case of the pseudosecond-order model (Figure 5). Also, in this case, the theoretically predicted equilibrium adsorption capacity was close to the experimentally determined value. The other models did not describe the kinetics of the adsorption process in a satisfactory manner, and the corresponding plots have therefore not been included here. This process was suitable for the description of the adsorption kinetics for the removal of As^V from aqueous solution onto Fe-XAD7-DEHPA resins. The adsorption can be seen as the rate-limiting step that controls the adsorption process. The rate constant k_2 increased with temperature increasing (Table 2), which shows that the process is endothermic.

As seen in Table 2, which shows the K_{dif} values and coefficient constant, the intraparticle diffusion model cannot be the dominating mechanism for the adsorption of the As^V from aqueous solution by the studied adsorbents.

Adsorption Thermodynamics. The rate constants k_2 calculated from eq 13 at different temperatures were used to estimate the activation energy of As^V onto Fe-XAD7-DEHPA resins. The rate constant is expressed as a function of temperature according to the well-known Arrhenius equation:[3,5,32,44,49]

$$\ln k_2 = \ln A - \frac{E^{\#}}{RT} \quad (15)$$

where $E^{\#}$ ($kJ \cdot mol^{-1}$) is the activation energy of adsorption, A is a constant called the frequency factor, and T and R have the same meanings as before. The activation energy $E^{\#}$ and the frequency factor A were calculated, respectively, from the slope and the intercept of the straight line obtained from the plot of $\ln K_2$ versus $1 \cdot T^{-1}/(1 \cdot K^{-1})$ as seen in Figure 6.

The magnitude of the activate energy $E^{\#}$ may provide a clue in the type of adsorption, physical or chemical.[2,44,49] The $E^{\#}$ values, calculated from the plot of ln k_2 versus $(1 \cdot T^{-1})/(1 \cdot K^{-1})$ (Figure 6), were found to be (7.012 and 6.21) $kJ \cdot mol^{-1}$ for the adsorption of As^V onto Fe-XAD7-DEHPA obtained through DM and CM, respectively. These values are of the same magnitude

Table 3. Thermodynamic Parameters for As^V Ion Adsorption onto Fe-XAD7-DEHPA Resins Obtained Through the Dry Method (DM) and the Column Method (CM)

T	k_2	$K^{\#}\cdot 10^{14}$	$\Delta H^{\#}$	$\Delta G^{\#}$	$\Delta S^{\#}$
K	$g\cdot mol^{-1}\cdot s^{-1}$	$g\cdot mol^{-1}$	$kJ\cdot mol^{-1}$	$kJ\cdot mol^{-1}$	$J\cdot mol^{-1}\cdot K^{-1}$
			DM		
298.15 ± 1	0.266	4.28	2.06	76.3	−249.0
303.15 ± 1	0.296	4.69	1.97	77.3	−249.0
318.15 ± 1	0.323	4.87	1.72	81.1	−249.4
			CM		
298.15 ± 1	0.303	4.88	1.26	75.9	−250.6
303.15 ± 1	0.319	5.05	1.17	77.1	−250.7
318.15 ± 1	0.356	5.37	0.92	80.8	−251.1

as the activation energy of the physisorption. The positive values of $E^{\#}$ indicate the endothermic nature of the adsorption process.

The relation between rate constant (k_2) and equilibrium constant ($K^{\#}$) can be given in the form:[49]

$$k_2 = \left(\frac{k_B\cdot T}{h}\right)\cdot K^{\#} \tag{16}$$

where $k_B = 1.381\cdot 10^{-23}\ J\cdot K^{-1}$ is the Boltzmann constant, $h = 6.626\cdot 10^{-34}\ J\cdot s$ is the Planck constant, and T is the absolute temperature. The value of $K^{\#}$ was calculated for each temperature for both studied adsorbents.

The relation between the activation energy and internal energy of activation ($\Delta U^{\#}$) can be derived by using the well-known Arrhenius ($d\ln k\cdot dT^{-1} = E^{\#}\cdot(RT^2)^{-1}$) and van't Hoff ($d\ln K^{\#}\cdot dT^{-1} = \Delta U^{\#}\cdot(RT^2)^{-1}$) equations in the temperature derivative of the last equation as follows:

$$d\ln\frac{k}{dT} = \left(\frac{1}{T}\right) + d\ln\frac{K^{\#}}{dT} \tag{17}$$

$$\frac{E^{\#}}{RT^2} = \left(\frac{1}{T}\right) + \frac{\Delta U^{\#}}{RT} \tag{18}$$

$$\Delta U^{\#} = E^{\#} - RT \tag{19}$$

The relation between the enthalpy ($\Delta H^{\#}$) and the internal energy of activation ($\Delta U^{\#}$) can be given in the form:

$$\begin{aligned}\Delta H^{\#} &= \Delta U^{\#} + \Delta v^{\#}RT \\ &= E^{\#} - RT + (1-m)RT = E^{\#} - mRT\end{aligned} \tag{20}$$

where $\Delta H^{\#}$ is the enthalpy of activation, $\Delta v^{\#} = 1 - m$ is the stoichiometric value of the activation reaction, and m is the molecularity, which is equal to the order.

The $\Delta H^{\#}$ value for each temperature was calculated from the last equation. The Gibbs energy for activation ($\Delta G^{\#}$) and entropy of activation ($\Delta S^{\#}$) were calculated from the equation:

$$\Delta G^{\#} = \Delta H^{\#} - T\Delta S^{\#} = -RT\ln K^{\#} \tag{21}$$

All of the thermodynamic parameters for the adsorption of As^V onto Fe-XAD7-DEHPA resins, obtained via DM and CM, are presented in Table 3.

As can be seen from Table 3, the positive $\Delta G^{\#}$ values indicate that the instability activation complex of the adsorption reaction increases with increasing temperature. Also, the positive $\Delta H^{\#}$ indicates the endothermic nature of adsorption at $T = (298.15 \pm 1$ to $318.15 \pm 1)$ K. The values of the negative activation entropy $\Delta S^{\#}$ confirm the decreased randomness at the solid−solution interface during adsorption.

CONCLUSIONS

XAD7-DEHPA resins were prepared through the DM and the CM. The both resins were loaded with iron to be used as adsorbents in the removal process of arsenate anions from aqueous solutions. The ability of the Fe-XAD7-DEHPA resins to remove As^V was examined, including equilibrium, kinetic, and thermodynamic studies of adsorption. Experiments were performed as a function of time, temperature, and initial concentration of As^V from solution.

The Langmuir, Freundlich, Temkin, and Dubinin−Kaganer−Radushkevich adsorption models were used for the mathematical explanations of the adsorption equilibrium of As^V. The R^2 values indicated that the adsorption of As^V onto Fe-XAD7-DEHPA fit the Langmuir and DKR isotherm model. The maximum adsorption capacities of Fe-XAD7-DEHPA obtained via DM and CM for As^V were (17 and 18) $\mu g\cdot g^{-1}$, respectively, obtained from the DKR isotherm model, which provided the best estimated error values.

The pseudofirst-order and pseudosecond-order kinetic and intraparticle diffusion models were used to model the adsorption of the As^V onto Fe-XAD7-DEHPA resins. It was determined that the interactions could be explained on the basis of the second-order kinetic model. The kinetic studies at the initial As^V concentration showed that the greatest adsorption capacity was achieved in 10 h of contact for the both studied materials.

The activation energies of As^V over the Fe-XAD7-DEHPA obtained through DM and CM were calculated as (7.012 and 6.21) $kJ\cdot mol^{-1}$, respectively. The positive values of $E^{\#}$ indicate that the adsorption process is an endothermic process of a physical nature.

The above results confirmed the potential of Fe-XAD7-DEHPA resins, obtained through DM and CM, as an adsorbent for As^V as well as other adsorbate. The adsorption capacities of the both studied materials are almost the same, but we can conclude that the Fe-XAD7-DEHPA obtained through the column method is most advantageous because this is obtained in a shorter time than the resin obtained via the DM.

AUTHOR INFORMATION

Corresponding Author

*Tel./Fax: +4 0256 404192. E-mail address: lavinia.lupa@chim.upt.ro.

Funding Sources

This work was supported by CNCSIS-UEFISCDI, Project No. PN II-IDEI 927/2008, "Integrated Concept about Depollution of Waters with Arsenic Content, through Adsorption on Oxide Materials, followed by Immobilization of the Resulted Waste in Crystalline Matrices". This work was partially supported by the strategic grant POSDRU/89/1.5/S/57649, Project ID 57649 (PERFORM-ERA), cofinanced by the European Social Fund—Investing in People, within the Sectoral Operational Programme, Human Resources Development, 2007−2013.

REFERENCES

(1) Kundu, S.; Gupta, A. K. Adsorptive removal of As(III) from aqueous solution using iron oxide coated cement (IOCC): Evaluation of kinetic, equilibrium and thermodynamic models. *Sep. Purif. Technol.* **2006**, *51*, 165–172.

(2) Borah, D.; Satokawa, S.; Kato, S.; Kojima, T. Surface-modified carbon black for As(V) removal. *J. Colloid Interface Sci.* **2008**, *319*, 53–62.

(3) Borah, D.; Satokawa, S.; Kato, S.; Kojima, T. Sorption of As(V) from aqueous solution using acid modified carbon black. *J. Hazard. Mater.* **2009**, *162*, 1269–1277.

(4) Negrea, A.; Lupa, L.; Ciopec, M.; Lazau, R.; Muntean, C.; Negrea, P. Adsorption of As(III) ions onto iron-containing waste sludge. *Adsorpt. Sci. Technol.* **2010**, *28*, 467–484.

(5) Ramesh, A.; Hasegawa, H.; Maki, T.; Ueda, K. Adsorption of inorganic and organic arsenic from aqueous solution by polymeric Al/Fe modified montmorillonite. *Sep. Purif. Technol.* **2007**, *56*, 90–100.

(6) Goswami, R.; Deb, P.; Thakur, R.; Sarma, K. P.; Bsumalick, A. Removal of As(III) from aqueous solution using functionalized ultrafine iron oxide nanoparticles. *Sep. Sci. Technol.* **2011**, *46*, 1017–1022.

(7) Ahmad, R. A.; Awwad, A. M. Thermodynamics of As(V) adsorption onto treated granular zeolitic tuff from aqueous solutions. *J. Chem. Eng. Data* **2010**, *55*, 3170–3173.

(8) Banerjee, K.; Amy, G. L.; Prevost, M.; Nour, S.; Jekel, M.; Gallagher, P. M.; Blumenschein, C. D. Kinetic and thermodynamic aspects of adsorption of arsenic onto granular ferric hydroxide (GFH). *Water Res.* **2008**, *42*, 3371–3378.

(9) Gupta, K.; Ghosh, U. C. Arsenic removal using hydrous nanostructure iron(III)-titanium(IV) binary mixed oxide from aqueous solution. *J. Hazard. Mater.* **2009**, *161*, 884–892.

(10) Hlavay, J.; Polyak, K. Determination of surface properties of iron hydroxide coated alumina adsorbent prepared from drinking water. *J. Colloid Interface Sci.* **2005**, *284*, 71–77.

(11) Nguyen, V. T.; Vigneswaran, S.; Ngo, H. H.; Shon, H. K.; Kandasamy, J. Arsenic removal by a membrane hybrid filtration system. *Desalination* **2009**, *236*, 363–369.

(12) Partey, F.; Norman, D.; Ndur, S.; Nartey, R. Arsenic sorption onto laterite iron concretions: Temperature effect. *J. Colloid Interface Sci.* **2008**, *321*, 493–500.

(13) Hsu, J. C.; Lin, C. J.; Liao, C. H.; Chen, S. T. Removal of As(V) and As(III) by reclaimed iron-oxide coated sands. *J. Hazard. Mater.* **2008**, *153*, 817–826.

(14) Chen, Y. N.; Chai, L. Y.; Shu, Y. D. Study of arsenic(V) adsorption on bone char from aqueous solution. *J. Hazard. Mater.* **2008**, *160*, 168–172.

(15) Bilici Baskan, M.; Pala, A. Determination of arsenic removal efficiency by ferric ions using response surface methodology. *J. Hazard. Mater.* **2009**, *166*, 796–801.

(16) Parga, J. R.; Cocke, D. L.; Valenzuela, J. L.; Gomes, J. A.; Kesmez, M.; Irwin, G.; Moreno, H.; Weir, M. Arsenic removal via electrocoagulation from heavy metal contaminated groundwater in La Comarca Lagunera Mexico. *J. Hazard. Mater.* **2005**, *B124*, 247–254.

(17) Bissen, M.; Frimmel, F. H. Arsenic-a review. Part II: oxidation of arsenic and its removal in water treatment. *Acta Hydrochim. Hydrobiol.* **2003**, *31*, 97–107.

(18) Song, S.; Lopez-Valdivieso, A.; Hernandez-Campos, D. J.; Peng, C.; Monroy-Fernandez, M. G.; Razo-Soto, I. Arsenic removal from high-arsenic water by enhanced coagulation with ferric ions and coarse calcite. *Water Res.* **2006**, *40*, 364–372.

(19) Wang, L.; Chen, A. S. C.; Sorg, T. J.; Fields, K. A. Field evaluation of As removal by IX and AA. *J. Am. Water Works Assoc.* **2002**, *94*, 161–173.

(20) Monah, D.; Pittman, C. U. Arsenic removal from water/wastewater using adsorbents- a critical review. *J. Hazard. Mater.* **2007**, *142*, 1–53.

(21) Jonsson, J.; Sherman, D. M. Sorption of As(III) and As(V) to siderite, green rust (fougerite) and magnetite; Implications for arsenic release in anoxic groundwaters. *Chem. Geol.* **2008**, *255*, 173–181.

(22) Ohe, K.; Tagai, Y.; Nakamura, S.; Oshima, T.; Baba, Y. Adsorption behaviour of arsenic(III) and arsenic(V) using magnetite. *J. Chem. Eng. Jpn.* **2005**, *38*, 671–676.

(23) Jeong, Y.; Fan, M.; Singh, S.; Chuang, C. L.; Saha, B.; van Leeuwen, J. H. Evaluation of iron oxide and aluminium oxide as potential arsenic(V) adsorbents. *Chem. Eng. Process* **2007**, *46*, 1030–1039.

(24) Gupta, K.; Basu, T.; Ghosh, U. C. Sorption characteristics of arsenic(V) for removal from water using agglomerated nanostructure iron(III)−zirconium(IV) bimetal mixed oxide. *J. Chem. Eng. Data* **2009**, *54*, 2222–2228.

(25) Ren, Z.; Zhang, G.; Chen, J. P. Adsorptive removal of arsenic from water by an iron-zirconium binary oxide adsorbent. *J. Colloid Interface Sci.* **2011**, *358*, 230–237.

(26) Maji, S. K.; Pal, A.; Pal, T. Arsenic removal from real-life groundwater by adsorption on laterite soil. *J. Hazard. Mater.* **2008**, *151*, 811–820.

(27) So, H. U.; Postma, D.; Jakobsen, R.; Larsen, F. Sorption and desorption of arsenate and arsenite on calcite. *Geochim. Cosmochim. Acta* **2008**, *72*, 5871–5884.

(28) Mondal, P.; Majumder, C. B.; Mohanty, B. Effects of adsorbent dose, its particle size and initial arsenic concentration on the removal of arsenic, iron and manganese from simulated ground water by FeIII impregnated activated carbon. *J. Hazard. Mater.* **2008**, *150*, 695–702.

(29) Chakraborty, A.; Saha, B. B.; Ng, K. C.; Koyama, S.; Srinivasan, K. Theoretical insight of physical adsorption for a single component adsorbent+adsorbate system: II The Henry region. *Langmuir* **2009**, *25*, 7359–7367.

(30) Belkhouche, N. E.; Didi, M. A. Extraction of Bi(III) from nitrate medium by D2EHPA impregnated onto Amberlite XAD-1180. *Hydrometallurgy* **2010**, *103*, 60–67.

(31) Chabani, M.; Amrane, A.; Bensmaili, A. Kinetics of nitrates adsorption on Amberlite IRA-400 resin. *Desalination* **2007**, *206*, 560–567.

(32) Hosseini-Bandegharaei, A.; Hosseini, M. S.; Sarw-Ghadi, M.; Zowghi, S.; Hosseini, E.; Hosseini-Bandegharaei, H. Kinetics, equilibrium and thermodynamic study of Cr(VI) sorption into toluidine blue o-impregnated XAD-7 resin beads and its application for the treatment of wastewaters containing Cr(VI). *Chem. Eng. J.* **2010**, *160*, 190–198.

(33) Mustafa, S.; Shah, K. H.; Naeem, A.; Waseem, M.; Tahir, M. Chromium (III) removal by weak acid exchanger Amberlite IRC-50 (Na). *J. Hazard. Mater.* **2008**, *160*, 1–5.

(34) Saha, B.; Gill, R. J.; Bailey, D. G.; Kabay, N.; Arda, M. Sorption of Cr(VI) from aqueous solution by Amberlite XAD-7 resin impregnated with Aliquat 336. *React. Funct. Polym.* **2004**, *60*, 223–244.

(35) Shao, W.; Li, X.; Cao, Q.; Luo, F.; Li, J.; Du, Y. Adsorption of arsenate and arsenite anions from aqueous medium by using metal (III)-loaded Amberlite resins. *Hydrometallurgy* **2008**, *91*, 138–143.

(36) Zhu, X.; Jyo, A. Removal of arsenic(V) by zirconium(IV)-loaded phosphoric acid chelating resin. *Sep. Sci. Technol.* **2001**, *36*, 3175–3189.

(37) Chanda, M.; O'Driscoll, K. F.; Rempel, G. L. Ligand exchange sorption of arsenate and arsenite anions by chelatin resins in ferric ion form: II. Iminodiacetic chelatin resin Chelex 100. *React. Polym.* **1988**, *8*, 85–95.

(38) An., B.; Steinwinder, T. R.; Zhao, D. Selective removal of arsenate from drinking water using a polymeric ligand exchanger. *Water Res.* **2005**, *39*, 4993–5004.

(39) Mendoza, R. N.; Medina, I. S.; Vera, A.; Rodriguez, M. A. Study of the sorption of Cr(III) with XAD-2 resin impregnated with di-(2,4,4-trimethylpentyl)phosphinic acid (Cyanex 272). *Solvent Extr. Ion Exch.* **2000**, *18*, 319–343.

(40) Muraviev, D.; Ghantous, L.; Valiente, M. Stabilization of solvent impregnated resin capacities by different techniques. *React. Funct. Polym.* **1998**, *38*, 259–268.

(41) Juang, R. S. Preparation, properties and sorption behaviour of impregnated resin containing acidic organophosphorus extractants. *Proc. Natl. Sci. Counc. ROC(A)* **1999**, *23*, 353–364.

(42) Benamor, M.; Bouariche, Z.; Belaid, T.; Draa, M. T. Kinetic studies on cadmium ions by Amberlite XAD7 impregnated resin containing di(2-ethylhexyl) phosphoric acid as extractant. *Sep. Purif. Technol.* **2008**, *59*, 74–84.

(43) Guo, X.; Fuhua, C. Removal of arsenic by bead cellulose loaded with iron oxyhydroxide from groundwater. *Environ. Sci. Technol.* **2005**, *39*, 6808–6818.

(44) Ada, K.; Ergene, A.; Tan, S.; Yalcin, E. Adsorption of Remazol Brilliant Blue R using ZnO fine powder: equilibrium, kinetic and thermodynamic modelling studies. *J. Hazard. Mater.* **2009**, *165*, 637–644.

(45) Mohad Din, A. T.; Hameed, B. H. Adsorption of methyl violet dye on acid modified activated carbon: isotherms and thermodynamics. *J. Appl. Sci. Environ. Sanit.* **2010**, *5*, 161–170.

(46) Lv, L.; He, J.; Wei, M.; Evans, D. G.; Zhou, Z. Treatment of high fluoride concentration water by MgAl-CO_3 layered double hydroxides: Kinetic and equilibrium studies. *Water Res.* **2007**, *41*, 1534–1542.

(47) El-Kamash, A. M.; Zaki, A. A.; Abdel, M.; Geleel, E. Modeling batch kinetics and thermodynamics of zinc and cadmium ions removal from waste solutions using synthetic zeolite. *J. Hazard. Mater.* **2005**, *B127*, 211–220.

(48) Allen, S. J.; Mckay, G.; Porter, J. F. Adsorption isotherm models for basic dye adsorption by peat in single and binary component systems. *J. Colloid Interface Sci.* **2004**, *280*, 322–333.

(49) Yu, Z.; Qi, T.; Qu, J.; Wang, L.; Chu, J. Removal of Ca(II) and Mg(II) from potassium chromate solution on Amberlite IRC 748 synthetic resin by ion exchange. *J. Hazard. Mater.* **2009**, *167*, 406–412.